Pseudopolarography of trace metals

ARTICLE *in* JOURNAL OF ELECTROANALYTICAL CHEMISTRY · FEBRUARY 2003

Impact Factor: 2.73 · DOI: 10.1016/S0022-0728(02)01484-5

2 AUTHORS, INCLUDING:

Dario Omanović
Ruđer Bošković Institute
70 PUBLICATIONS **664** CITATIONS

Available online at www.sciencedirect.com
SCIENCE DIRECT®
Journal of Electroanalytical Chemistry 543 (2003) 83–92
Journal of Electroanalytical Chemistry
www.elsevier.com/locate/jelechem

Pseudopolarography of trace metals Part I. The automatic ASV measurements of reversible electrode reactions

Dario Omanović *, Marko Branica

Center for Marine and Environmental Research Zagreb, Ruđer Bošković Institute, PO Box 180, 10002 Zagreb, Croatia

Received 20 September 2002; received in revised form 6 November 2002; accepted 18 November 2002

Abstract

The main advantage of automated computer-controlled pseudopolarographic measurements is the possibility of their practical application to the determination of trace metal speciation. This paper describes the pseudopolarographic characteristics of the reversible electrochemical reactions of dissolved trace metals, such as: lead(II), thallium(I) and bismuth(III), in model electrolytes, at a metal concentrations of about 10^{-7} mol l^{-1}, on a stationary mercury drop electrode (SMDE), using a differential pulse anodic stripping voltammetry (DPASV) technique. There is good agreement between the formal potential determined by the sampled dc polarography (10^{-4} mol l^{-1}) and pseudopolarography (10^{-7} mol l^{-1}). The half-wave potential of the pseudopolarograms shifts with the accumulation time but remains unaffected by the increase of the metal concentration in the solution, which is in good agreement with the theoretical suppositions. The dependence of the shape of the pseudopolarogram on the method used for the determination of the anodic peak current, is presented. The development and the application of an efficient mathematical treatment of the experimental (pseudo)polarographic data for the determination of the half-wave potential, the transfer coefficient, the rate constant, etc., are presented.

Keywords: Anodic stripping voltammetry; Automation; Data simulation; Data treatment; Polarography; Pseudopolarography; Speciation; Trace metals

1. Introduction

Pseudopolarography (also known as a neopolarography) is an electroanalytical method which is used for the determination of the trace metal speciation, at a very low dissolved metal concentrations, in various model electrolytes and natural waters. This method was introduced about thirty years ago [1–4], and is based on the anodic stripping voltammetry (ASV) technique: a series of voltamograms are obtained by the consecutive changes of the accumulation potential, [1,2]. The curve constructed from the anodic peak currents versus accumulation potentials, appears like a classical dc polarogram, and is called a pseudopolarogram.

A theory of pseudopolarography has already been developed for a mercury drop electrode (MDE) [3,4], a thin mercury film (TMF) electrode [5], and an ultra microelectrode (UME) [6]. An improvement on the theory for a TMF electrode was made [7], for which the basic principles can also be applied to a MDE.

The first approach to pseudopolarographic measurements was based on manual operation, which is very time-consuming and complicated. This is probably the reason that only a small number of papers containing the experimental results of the speciation of trace metals at the actual concentration levels in natural waters, was published. However, it was shown that pseudopolarography can successfully be applied to the characterisation of labile [1,2,8–17] and inert [16–20] complexes at

* Corresponding author. Fax: +385-1-4680-231.
E-mail address: omanovic@rudjer.irb.hr (D. Omanović).

0022-0728/02/$ - see front matter
doi:10.1016/S0022-0728(02)01484-5

low metal concentration levels ($<10^{-7}$ mol l^{-1}). The stability constants of the labile metal complexes obtained by pseudopolarography are in very good agreement with the literature data obtained at much higher metal concentration levels [2,11–14] using other 'classical' methods, such as polarography and spectrometry. The common problem of the precipitation of the hydrolized species at higher metal concentration levels ($>10^{-4}$ mol l^{-1}), can be overcome by using a pseudopolarographic approach. Most of the metals will be dissolved if the measurements are performed at a few orders of magnitude lower concentration levels. The results of the application of pseudopolarography for the characterisation of reversible labile complexes [1,2,5,11], as well as quasireversible electrochemical processes [12–14], are published elsewhere.

Some authors used pseudopolarography for the speciation of inert metal complexes, both in model solutions [16–18] and natural water samples [19,20]. It was shown that the inert complexes were irreversibly reduced at more negative potentials than the free metal/labile metal complexes, and in some cases, the values of the stability constants were estimated [18–20].

A half-wave potential and a limiting current which are extracted from the pseudopolarographic curves, are the main parameters for the determination of the metal speciation. For quasireversible or irreversible electrochemical reactions, the transfer coefficient and the rate constant can also be evaluated. The efficient mathematical treatment of the raw pseudopolarographic/voltammetric data leads to a satisfactory final result.

The automation of the pseudopolarographic measurements enables numerous applications of this method to the systematic investigations of trace metal speciation [15,21]. The first detailed description of automated pseudopolarographic measurements using a EG&G polarographic analyser PAR 384B with a PAR 303 SMDE connected to the HP 9816-S technical computer, appeared about 15 years ago [15]. The version for PC-compatible computers with a new graphical interface and the mathematical routines added for data treatment, was described a few years ago [21].

In this paper some fundamental principles of the pseudopolarography of trace metals on the mercury drop electrode using the automated measurement system consisting of new software, PSEUDOSOFT, and an AUTOLAB instrument, are described in detail. The theoretical relationships of the pseudopolarography of trace metals, unpublished so far, are verified experimentally. The experimental dependences of the pseudopolarographic curves of the reversible (one-, two- and three-electron charge transfer) electrochemical reaction of trace metals, as well as the experimental problems, which occurred during the measurements, are presented. These problems can be solved successfully by the use of the procedure presented.

2. Experimental

The pseudopolarographic, voltammetric, polarographic and amperometric measurements were performed using a μAUTOLAB multimode polarograph (EcoChemie, Utrecht, The Netherlands) connected to a PC computer. The automatic pseudopolarographic measurements were carried out using a newly developed software called PSEUDOSOFT [22]. The μAUTOLAB polarographic operations were controlled by the main programme module using a modified version of Electro-Analytical System software version 2.4 (EAS). This software enabled continuous experimental measurements for several days and the possibility of the change of the supporting electrolyte composition using the automatic burette system (Cavro, San Jose, USA).

An electrochemical cell with a three-electrode system was used in all measurements. The working electrode was a static mercury drop electrode (SMDE) PAR 303A with a modified holder of the electrode components [23]. The reference electrode was an Ag | AgCl | sat. NaCl electrode, and a platinum wire was used as a counter electrode. The electrolyte solution was stirred at 4000 rpm using a quartz rotating stirrer driven by a 'Port Escap DC' electromotor controlled by a home-made power supply. The pH of the solution was controlled by an Orion Research pH meter (EA 920) with a glass pH electrode. Prior to measurements, the electrolytes in the electrochemical cell were purged with extra-pure nitrogen for 15 min; a nitrogen blanket was maintained thereafter.

Differential pulse anodic stripping voltammetry (DPASV) and sampled dc polarography, as scanning operating modes, were applied under selected conditions of: a deposition potential (E_{dep}), an initial potential (E_i), a final potential (E_f), a differential pulse amplitude (A), a potential step increment ($E_{st\ inc}$), an accumulation time (t_{acc}), a time between pulses (t_{int}), a pulse duration (t_{dur}) and a drop time (t_d).

All electrolyte solutions were prepared using Milli-Q water. The chemicals used were either of 'suprapur' (concentrated $HClO_4$ and HNO_3) or of 'analytical-reagent' grade, $Bi(NO_3)_3$ (Fluka, Buchs), $Pb(NO_3)_2$, $TlNO_3$, $NaClO_4 \times H_2O$ and NaCl (Merck, Darmstadt).

The blank concentration of the dissolved trace metals (mainly lead) in the supporting electrolyte was diminished by potentiostatic electrolysis (reduction) using an EG&G potentiostat model PAR 273. The electrochemical purification cell comprised a three electrode system: the working electrode was a mercury pool (64 cm^2), the reference electrode was Ag | AgCl | sat. NaCl and a platinum wire was used as a counter electrode (5 cm^2). Prior to electrolysis through 0.22 and 0.05 m Millipore filters, the solution (0.5 l) was pretreated overnight with active carbon and filtered. The electrolysis was carried

out at the potential of −1.25 V for at least 4 h under an N_2-atmosphere.

3. Results and discussion

A standard redox potential (E°/V) is commonly used in thermodynamical calculations. However, for practical reasons, it is frequently substituted by a formal potential ($E^{\circ\prime}$/V) [25]. This is a value which depends on the conditions existing in the electrolyte, such as ionic strength, complexation ligands, etc. Hence, the theoretical models developed on the basis of the formal potential are more useful in the evaluation of the experimental results. In this work, the simulations of the polarographic [24] and pseudopolarographic [4] curves are based on the formal potential as a reference value. The formal potentials obtained experimentally, are expected to be practically equal for both methods. This was tested by the measurements of Pb (10^{-4} and 10^{-7} M) performed in 0.1 mol l^{-1} $NaClO_4$ electrolyte, pH < 2.

3.1. Polarographic and amperometric measurements

The formal potential and diffusion coefficient of Pb(II) ions were determined from the polarographic measurements. The well-known Cottrell equation [25] can be applied to the limiting current controlled by diffusion, in order to calculate the diffusion coefficients from the currents obtained at constant potential. In polarography, this condition is fulfilled only if a static mercury drop electrode (SMDE) and a sampled dc scanning technique are utilized. For the mercury drop electrode, the original Cottrell-equation must be extended by a factor which includes the spherical form of the drop [25,26]:

$$I = nFSc_0^*[(D/\pi t_d)^{1/2} + (D/r)] \quad (1)$$

where I is the current, n the number of electrons, F the Faraday constant, S the area of the mercury drop, c_0^* the concentration of the electroactive species in the bulk of the solution, D the diffusion coefficient, t_d the drop time and r the radius of the mercury drop.

Fig. 1 shows the experimental polarograms of 1×10^{-4} mol l^{-1} Pb(II) with varied drop times. However, the expected linear correlation of the limiting currents with the reciprocal values of the square root of the drop time (the 'time between drops'), was not obtained. The Cottrell-equation and its extended version imply that the drop has formed (with a constant area) at the beginning of the constant potential step. In our case, this condition is not fulfilled because of the duration required for the formation of the drop. This problem also appears in the literature. According to the experimentally obtained

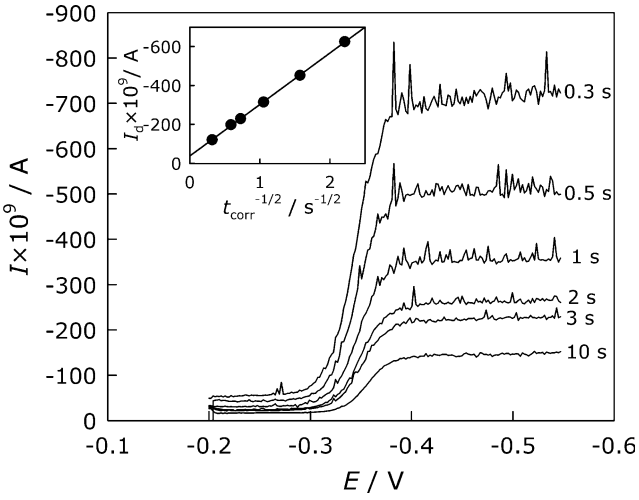

Fig. 1. The sampled dc polarograms of a 1×10^{-4} mol l^{-1} Pb(II) in the supporting electrolyte of 0.1 mol l^{-1} $NaClO_4$, pH < 2, at different 'times between drop'. Inset: The dependence of the limiting current on the reciprocal value of the square root of the corrected drop time (t_{corr}).

results of Bond and Jones [26], Anderson et al. [27] and Gonzalez-Arjona et al. [28], the following total times required for the drop formation at a PAR 303 A SMDE were found: small, 117 ms; medium, 167 ms; and large, 267 ms. It is obvious that the drop time from the Cottrell-equation must be corrected, i.e. replaced by the 'duration of the drop'. Therefore, a correction factor (t_{form}) must be included in the extended Cottrell-equation:

$$I = nFSc_0^*[(D/\pi(t_d - t_{form}))^{1/2} + (D/r)] \quad (2)$$

The correction factor (t_{form}) and the diffusion coefficient of the Pb(II) ions were computed by fitting the experimental data to the equation:

$$I = 10^{-4}D^{1/2}(t_d - t_{form})^{-1/2} + 6.56\times10^{-3}D \quad (3)$$

The following experimental data were obtained: the diffusion coefficient of the Pb(II) ions, $D = 0.66 \times 10^{-5}$ cm^2 s^{-1}, and the correction factor, $t_{form} = 106$ ms. The correction factor (106 ms) is in good agreement with the values derived from the data published elsewhere (117 ms). The linear relationship of the limiting currents on the reciprocal values of the square root of the corrected drop time was obtained (inset in Fig. 1). The formal potential was determined by comparing the simulated and experimental polarograms. The diffusion coefficient of the lead in mercury (amalgam) was taken from the literature [29] ($D_{Pb(Hg)} = 2.1 \times 10^{-5}$ cm^2 s^{-1}). Prior to the simulation, the polarograms were treated as follows: (1) a linear baseline current was subtracted; and (2) the polarograms were normalized by dividing each point with its limiting current. All normalized polarograms showed practically the same curves, which is predictable theoretically for the reversible two-electron redox reac-

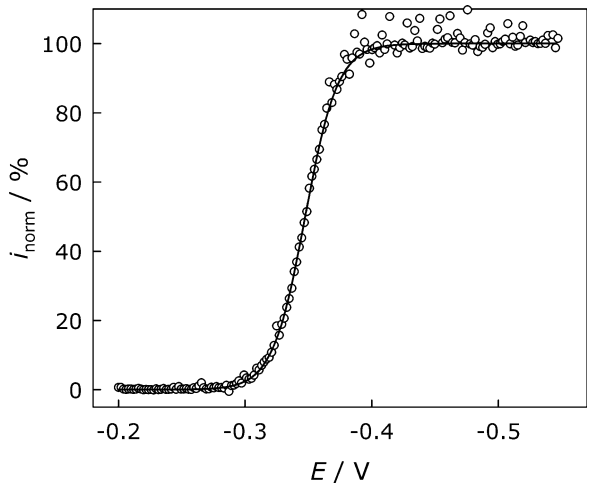

Fig. 2. The normalized experimental (○) and simulated (—) sampled dc polarograms of 1×10^{-4} mol l^{-1} Pb(II) in the supporting electrolyte of a 0.1 mol l^{-1} $NaClO_4$, pH < 2, at a 'time between drops' of 1 s. The simulation parameters: $t_d = 1$ s, $D_{ox} = 0.66 \times 10^{-5}$ cm^2 s^{-1}, $D_{red} = 2.1 \times 10^{-5}$ cm^2 s^{-1}, $E^{\circ\prime} = -0.354$ V.

tion. The example of the experimental (circles) and simulated (full line) polarograms is shown in Fig. 2. The formal potential, evaluated by comparing these curves ($E^{\circ\prime} = -0.354$ V) versus the reference electrode (Ag | AgCl | sat. NaCl), valid only for the solution of 0.1 mol l^{-1} $NaClO_4$ and pH < 2, is given.

A diffusion layer thickness (δ) was also required for the simulation of the pseudopolarograms. It was determined amperometrically from the reduction currents of 1×10^{-3} mol l^{-1} Pb(II) in a stirred solution (0.1 mol l^{-1} $NaClO_4$, pH < 2) at the constant potential of –0.7 V. At this potential, the concentration of Pb^{2+} ions at the mercury surface was zero. A four orders of magnitude higher concentration of the Pb^{2+} ions, in comparison with the pseudopolarographic measurements, was used to increase the faradic part of the total current. Table 1 shows the values of the Pb(II) diffusion layer thickness (δ) for the three mercury drop sizes calculated using the following equation:

$$I = nFSDc_0^*/\delta \quad (4)$$

Table 1
The diffusion current (I_d) and diffusion layer thickness (δ) of 10^{-3} mol l^{-1} Pb(II) measured in stirred solution (0.1 mol l^{-1} $NaClO_4$, pH < 2) for the three mercury drop sizes

	I_d/μA		
	Small (0.00921 cm^2)	Medium (0.0155 cm^2)	Large (0.0264 cm^2)
'Blank'	0.303	0.521	0.868
10^{-3} mol l^{-1} Pb^{2+}	14.874	24.007	39.814
Net current/μA	14.571	23.486	38.946
$\delta \times 10^3$/cm	0.81	0.84	0.86

The following parameters required for the simulation of the pseudopolarograms in the solution of a 0.1 mol l^{-1} $NaClO_4$, pH < 2 were determined:

r_{drop}: 0.0271 cm (0.00921 cm^2)
D_{ox}: 0.66×10^{-5} cm^2 s^{-1}
D_{red}: 2.1×10^{-5} cm^2 s^{-1}
δ: 0.81×10^{-3} cm
$E^{\circ\prime}$: −0.354 V

3.2. Pseudopolarographic measurements

3.2.1. Variation of accumulation time

The automatic pseudopolarographic measurements were carried out using newly developed computer software PSEUDOSOFT. Fig. 3A illustrates the original pseudopolarograms of 2×10^{-7} mol l^{-1} Pb(II) for

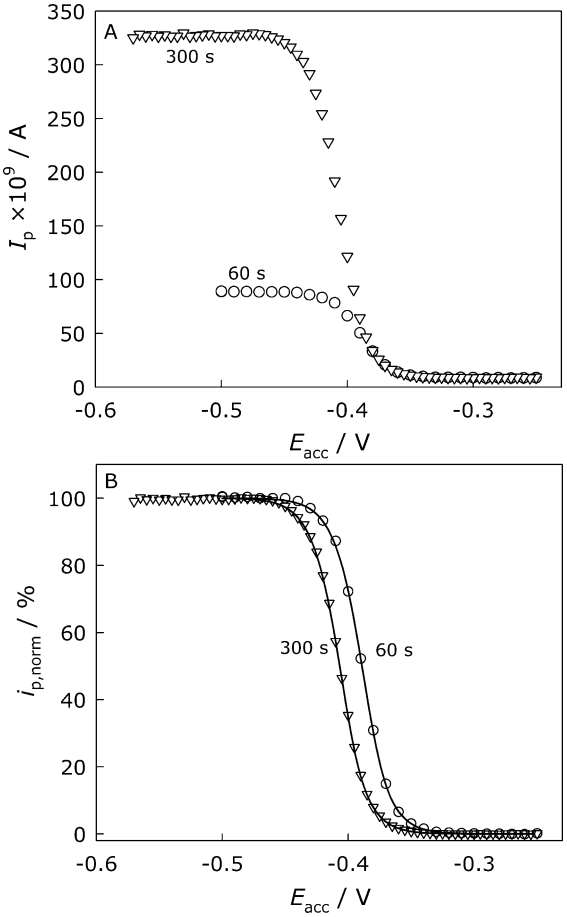

Fig. 3. The original (A) and normalized (B) experimental pseudopolarograms of 2×10^{-7} mol l^{-1} Pb(II) in the supporting electrolyte of a 0.1 mol l^{-1} $NaClO_4$, pH < 2, at two accumulation times, (○) 60 s and (▽) 300 s. The full line represents simulated pseudopolarograms. The DPASV parameters: $E_i = -0.55$ V, $E_f = -0.20$ V, $E_{sc.inc} = -0.002$ V, $E_A = 0.025$ V, $t_{int} = 0.2$ s, $t_{mod} = 0.05$ s. The simulation parameters: $t_{acc} = 49$ and 198 s, $\delta = 0.81 \times 10^{-3}$ cm, $D = 0.66 \times 10^{-5}$ cm^2 s^{-1}, $E_{form} = -0.354$ V, $r_{drop} = 0.0271$ cm.

accumulation times of 60 and 300 s, respectively. All anodic stripping voltamograms of the Pb(II) showed reversible response with a peak potential of -0.357 ± 0.001 V. The experimental pseudopolarograms were treated in a manner described previously. The normalized pseudopolarograms are shown in Fig. 3B. However, the half-wave potentials of the experimental pseudopolarograms shifted to positive potentials as compared to the polarograms simulated using the formal potential, $E^{\circ\prime} = -0.354$ V (3.0 mV for $t_{acc} = 60$ s, and 5.5 mV for $t_{acc} = 300$ s).

A simplified equation of the half-wave potential for the reversible pseudopolarogram at the mercury drop electrode is given [4]:

$$E_{1/2} = E^{\circ\prime} + 0.059 \times \log(2r\delta/3Dt_{acc})/n \quad (5)$$

The difference between the half-wave potentials for the two accumulation times is represented by the equation:

$$E_{1/2,2} - E_{1/2,1} = 0.059 \times \log(t_{acc,1}/t_{acc,2})/n \quad (6)$$

According to the theory, the accumulation time can be replaced by the limiting current of the pseudopolarograms, which is a measure of the reoxidized amalgam [30]:

$$E_{1/2,2} - E_{1/2,1} = 0.059 \times \log(i_{lim,1}/i_{lim,2})/n \quad (7)$$

A linearity between the difference of the half-wave potentials and the logarithm of the limiting current ratio with a slope of $59/n$ mV, needs to be obtained. The same applies if the accumulation times are used instead of the limiting currents. However, the linearity of the limiting current and the accumulation time was not achieved experimentally on a mercury drop electrode (Fig. 4). The reason for the curvilinear dependence is a diminishing of the relative 'active' concentration of the amalgam in the mercury drop electrode available during the anodic stripping step (reoxidation of Pb(0)). This is mainly caused by the diffusion of the amalgam towards the middle of the drop and inside the capillary. The amalgam diffused further with a longer accumulation time, thus decreasing its relative concentration [31]. The linearity of the limiting current and the accumulation time was achieved only during the shorter accumulation time (< 40 s, Fig. 4). This range was used to approximate a straight line which represents the expected values of the limiting currents. If the experimental limiting currents for the accumulation times of 60 and 300 s, are translated to the straight line, the equivalent accumulation times are obtained: 49 and 198 s, respectively. A repeated simulation with the equivalent accumulation times shows an agreement between the experimental and the simulated pseudopolarograms (using the formal potential obtained by polarography).

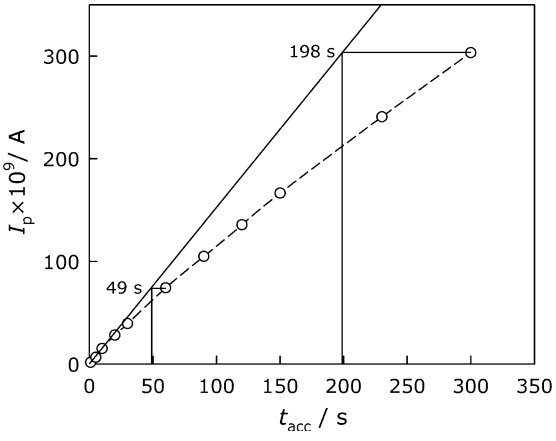

Fig. 4. The dependence of the anodic peak current of 2×10^{-7} mol l^{-1} Pb(II) in the supporting electrolyte of 0.1 mol l^{-1} $NaClO_4$, pH < 2, on the accumulation time. The DPASV parameters: $E_{acc} = -0.55$ V, $E_i = -0.55$ V, $E_f = -0.20$ V, $E_{sc.inc} = -0.002$ V, $E_A = 0.025$ V, $t_{int} = 0.2$ s, $t_{mod} = 0.05$ s.

In polarography, it is very important to point out that the concentrations of the reduced and oxidized metal forms at the half-wave potential, are almost equal (if both diffusion coefficients are similar). However, this is invalid for the pseudopolarographic half-wave potential, which is only a potential at the half of the maximal (limiting) current. In pseudopolarography, the ratio of the concentrations of the reduced and oxidized metal forms varies with the accumulation time, the diffusion layer thickness, the size of the mercury drop or the mercury film thickness, etc.

This example shows that, in some cases, a theoretical relationship can be achieved only with the additional correction of the experimental data. It also confirms the accuracy of the theory of pseudopolarography applied to the measurements on the mercury drop electrode [4] which is used for the simulations.

Additional experiments with five different accumulation times (30, 60, 120, 240 and 480 s), in 1 mol l^{-1} NaCl (pH < 2) supporting electrolyte confirmed such behaviour. The dependence of the formal potential on the logarithm of the equivalent accumulation time confirmed the reversibility of the redox process of Pb(II) with a slope of the straight line of 29 mV.

3.2.2. Variation of depolarizer concentration

In the example illustrated, the half-wave potential of the pseudopolarogram shifted to a more negative value with an increase of the accumulation time, i.e. the limiting current. In addition, the limiting current of the pseudopolarograms can increase with the addition of an electroactive substance (dissolved metal ions). Fig. 5A shows pseudopolarograms with increased concentrations of Pb(II) in 1 mol l^{-1} NaCl supporting electrolyte (pH < 2), at the accumulation time of 60 s. It is evident that the base current increases with the addition of the Pb(II) ions. These currents originate from the oxidation of the amalgams accumulated during the equilibration

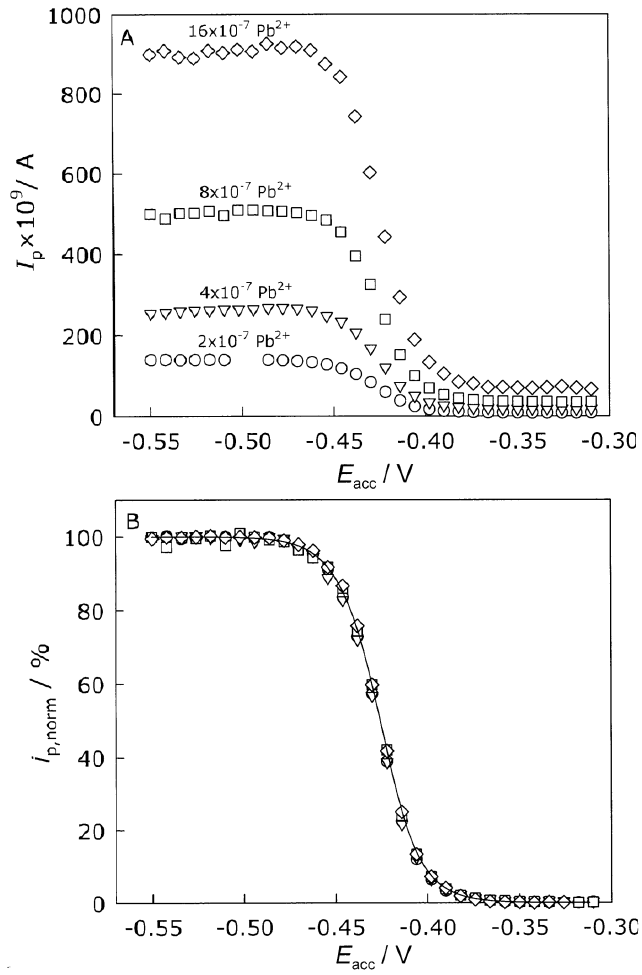

Fig. 5. The original (A) and normalized (B) experimental pseudopolarograms of (○) 2×10^{-7}, (▽) 4×10^{-7}, (□) 8×10^{-7}, (◇) 16×10^{-7} mol l^{-1} Pb(II) in the supporting electrolyte of a 1 mol l^{-1} NaCl, pH < 2, at the accumulation time of 60 s. The full line represents the simulated pseudopolarograms. The DPASV parameters: $E_i = -0.57$ V, $E_f = -0.25$ V, $E_{sc.inc} = -0.002$ V, $E_A = 0.025$ V, $t_{int} = 0.2$ s, $t_{mod} = 0.05$ s. The simulation parameters: $t_{acc} = 60$ s, $\delta = 0.81 \times 10^{-3}$ cm, $D = 0.66 \times 10^{-5}$ cm^2 s^{-1}, $E_{form} = -0.394$ V, $r_{drop} = 0.0351$ cm.

time and positive scan, and have the same relative increase as the limiting currents.

In contrast to the shift of the half-wave potential with an increase of the accumulation time at a constant concentration of the Pb(II) ions, no change of the half-wave potentials of the pseudopolarograms with the increase of the concentration of the Pb(II) ions, was observed (Fig. 5B). The minor difference was due to a very small deviation of the linearity of the peak current with the increase of the concentration of the Pb(II) ions. At each accumulation potential, the ratio of the reduced and the oxidized forms are equal for each concentration of the dissolved Pb(II) in the electrolyte solution. However, this ratio becomes higher with an increase of the accumulation time. Comparing the linearity of the limiting currents with the increase of both the accumulation time and the concentration of the Pb(II) ions, an assumption that the accumulated metal diffuses into the capillary during a longer accumulation time, can be confirmed.

3.2.3. 'Memory effect'

The term 'memory effect' has been introduced in the electroanalytical practice of the physico-chemical characterization of the trace metals. Such an effect occurs during repeated measurements when the subsequent data depend on the preceding data. Consequently, biased results are obtained. In pseudopolarography, each point is measured on a fresh mercury drop. During the accumulation time, a reduced form of the electroactive substance (amalgam) diffuses into the mercury drop and the capillary. In our measurements, a new 'active' drop was formed following 3–5 discarded mercury drops. It is assumed that such a procedure avoids the 'memory effect'. The measurements of the pseudopolarograms of 2×10^{-7} mol l^{-1} Pb(II) in 0.1 mol l^{-1} $NaClO_4$ (pH < 2) at two accumulation times, were performed in order to verify such an assumption. The direction of the accumulation potential was changed for the accumulation times of 60 and 300 seconds, respectively: first in the positive, and then in the negative direction. The pseudopolarograms were measured using a small mercury drop, i.e. a smaller ratio of a drop size and an inner capillary diameter ($r_{drop} = 0.0271$ cm, $(Ø/2)_{cap} = 0.005$ cm), which can enhance the potentially available 'memory effect'. The original pseudopolarograms were normalized as described previously. The results are presented in Fig. 6. The graph illustrates that the half-wave potential remains constant for both accumulation times, regardless of the change of the direction of the accumulation potential. The form of the pseudopolarograms also remained unchanged under these experimental conditions.

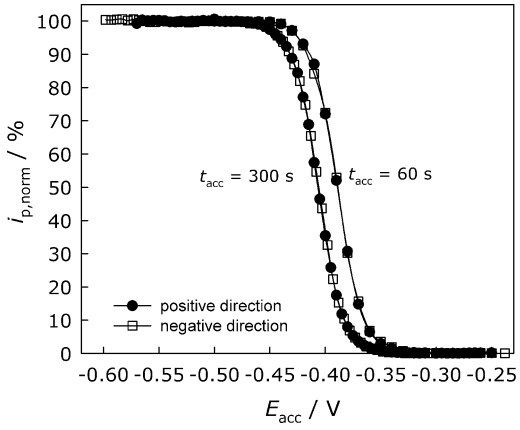

Fig. 6. The normalized pseudopolarograms of 2×10^{-7} mol l^{-1} Pb(II) in the supporting electrolyte of a 0.1 mol l^{-1} $NaClO_4$, pH < 2, at the accumulation times of 60 and 300 s, recorded in the positive (●) and the negative (□) direction of the change of the accumulation potential. The DPASV parameters: $E_i = -0.55$ V, $E_f = -0.20$ V, $E_{sc.inc} = -0.002$ V, $E_A = 0.025$ V, $t_{int} = 0.2$ s, $t_{mod} = 0.05$ s.

3.2.4. The shape of the limiting currents

The pseudopolarographic measurements of the Tl(I) as a one-electron charge transfer, were also performed. The DPAS voltamograms were recorded in an electrolyte solution of 0.1 mol l^{-1} $NaClO_4$, pH < 2, at a concentration of the Tl(I) of 1×10^{-7} mol l^{-1}. It is evident that the currents of the pseudopolarograms in the potential range between −0.60 and −0.85 V, are not constant, as predicted theoretically. The pseudopolarograms published elsewhere were either recorded in a relatively narrow range of the accumulation potentials, as compared with their half-wave potentials, or only a few points in the range of the limiting current (often dispersed) were taken into account. Therefore, it is rather difficult to resolve the shape of the limiting current from these pseudopolarograms. In several papers, the authors offer no explanation for the noticeable change of the limiting current. However, some authors speculated on such a behaviour: Seitz et al. [32] qualified it as a deterioration of the mercury surface by the accumulation of foreign metals, indicating a significant overpotential for the deposition, which seems probable for the measurements performed in a seawater sample; Huizenga and Kester [33] attributed such an effect to the loss of an intermediate species during the reduction step of the Pb(II) to Pb(0); Wang and Zadeii [34] described in their work with an ultra micro electrode (UME) that significant plating of the metal occurs during the scanning period as a result of the unique diffusional flux at the UME. Finally, Kounaves [6] found that the rise of the limiting current with the increase of the negative accumulation potential, was caused by the adsorption of organic matter (algae) originating from the cartridges of the deionised (DI) water supply. After changing the cartridges, a flat limiting current was obtained.

One may suppose that the rise of the limiting current of our experimental pseudopolarograms is the result of the adsorption of the unknown surface-active substance (SAS) on the surface of the mercury drop. The maximal adsorption of the various SAS takes place in the potential range between −0.2 and −1.0 V [35–37]. The adsorption weakens at potentials more positive or negative than this range. At the potentials of about 0 and −1.5 V, the SASs are mostly desorbed from the surface of the mercury drop [35]. The SASs adsorbed on the mercury surface prevent an effective reduction (and oxidation) of the trace metals, diminishing the anodic peak current. By changing the accumulation potential in a negative direction, the amount of the adsorbed SAS diminishes, causing the rise of the limiting current of the pseudopolarograms. Our experiments with zinc and cadmium performed in a wide potential range (−1.4 to −0.4 V; not presented here) show that the rise of the limiting current of the pseudopolarograms becomes higher with an increase of the supporting electrolyte concentration and the accumulation time. These experiments can verify the assumption that the SAS adsorbs on the mercury surface. The SAS in the supporting electrolyte probably originated from polluted sodium–perchlorate. It is known that the reduction of Tl(I) is not significantly affected by the adsorbed SAS as it is for cadmium, lead, copper, etc., but a small increase of the limiting current is evident (Fig. 7). The problem arises when the electrochemical parameters are evaluated from such curves (half-wave potential, transfer coefficient, rate constant). These parameters are usually evaluated by a logarithmic analysis of the polarographic or pseudopolarographic curves. However, in extreme situations, when the shape of the limiting current is considerably changed, a common logarithmic analysis yields no accurate results. If the process during which such (pseudo)polarogams are formed, is known, the corrections performed using the exact mathematical treatment, yield favourable results [38]. There are several forms of the (pseudo)polarograms with the inappropriate base and/or limiting currents, which can be obtained

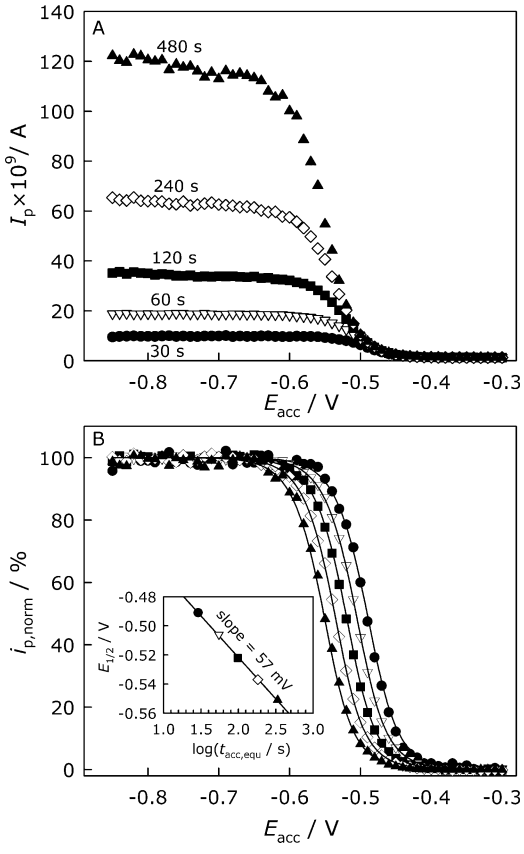

Fig. 7. The original (A) and normalized (B) pseudopolarograms of 2×10^{-7} mol l^{-1} Tl(I) in the supporting electrolyte of 0.1 mol l^{-1} $NaClO_4$, pH < 2, at different accumulation times 30, 60, 120, 240 and 480 s. The full lines represent simulated pseudopolarograms. The DPASV parameters: $E_i = -0.65$ V, $E_f = -0.20$ V, $E_{sc.inc} = -0.002$ V, $E_A = 0.025$ V, $t_{int} = 0.2$ s, $t_{mod} = 0.05$ s. The simulation parameters: $t_{acc} = 60$ s, $\delta = 1.4 \times 10^{-3}$ cm, $D = 1 \times 10^{-5}$ cm^2 s^{-1}, $E_{form} = -0.427$ V, $r_{drop} = 0.0351$ cm.

experimentally. Some of these, representing possible experimental curves, are illustrated in Fig. 8A by the simulated pseudopolarograms: curve 1—the original pseudopolarogram; curve 2—a pseudopolarogram with the addition of an increasing base current with a constant slope; and curve 3—a pseudopolarogram with an increasing slope of the base current, which affects the pseudopolarogram mostly at higher currents (> 10%). The treatment of curve 2 is very simple: a linear base line with a constant slope is subtracted from the whole curve, resulting in (pseudo)polarograms with a flat base and a limiting current. However, the treatment of curve 3 requires a different approach. A method for the data treatment is proposed in order to solve the problem. This method is derived from the 'method of the internal standard', which is based on the relation of the

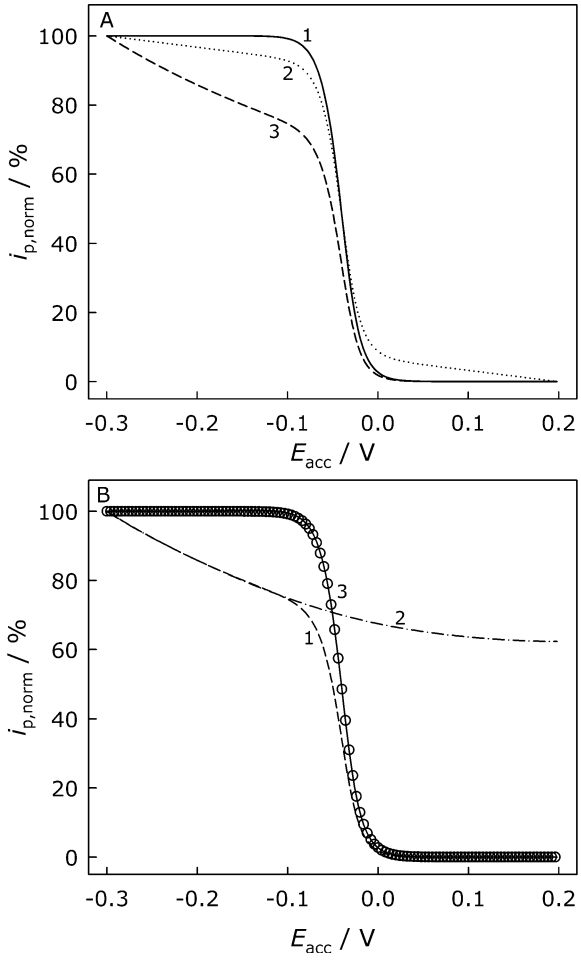

Fig. 8. (A) Simulated pseudopolarograms of the two-electron charge transfer with different base and limiting currents, (1) original curve, (2) curve with a constant slope of the base/limiting current and (3) curve with an increasing slope of the base/limiting currents. (B) Treatment of the simulated pseudopolarogram using the 'method of the internal standard', (1) curve with an increasing slope of the base/limiting current, (2) approximated limiting current, (3) treated curve. The empty circles correspond to the original pseudopolarogram. The simulation parameters: $t_{acc} = 60$ s, $\delta = 1.4 \times 10^{-3}$ cm, $D = 1 \times 10^{-5}$ cm^2 s^{-1}, $E_{form} = 0$ V, $r_{drop} = 0.0351$ cm.

investigated and introduced additional (internal standard) redox process [23]. The peak currents of the redox process investigated are divided from the peak currents of the 'internal standard'. In the derived method proposed (illustrated in Fig. 8B), the currents of the pseudopolarogram investigated (curve 1) are divided by the manually drawn approximated limiting current (curve 2), which represents an 'internal standard', and is in an agreement with the limiting current of the 'experimental' pseudopolarogram. The resulting pseudopolarogram (curve 3) is in good agreement with the original pseudopolarogram (empty circles or curve 1, Fig. 8A). It is essential that, prior to treatment, the base current of the pseudopolarogram needs to be near zero value. This simulated model confirms the validity of the approach proposed for the data treatment. The main problem that needs to be resolved is the drawing of an acceptable approximated limiting current where experience is of crucial importance. Most of our experimental pseudopolarograms obtained using various trace metals and electrolyte compositions, are in the shape of the limiting current (curve 3 in Fig. 8A). This method is used for the treatment of the pseudopolarograms of Tl(I) presented in Fig. 7B. By the correction of the accumulation time, the linear relationship of the half-wave potential to the equivalent accumulation time with a slope of 57.1 mV was obtained (inset in Fig. 7B). This is in good agreement with the theoretically predicted value for a reversible one-electron charge transfer (59 mV).

3.2.5. The peak current determination

In the electroanalytical determination of the dissolved trace metal concentrations, an accurate peak current estimate is very important [39]. The same applies to the pseudopolarographic measurements. Fig. 9 shows the DPAS voltamograms of 2×10^{-7} mol l^{-1} Bi(III) with different chloride concentrations in the supporting electrolyte: 5×10^{-3} mol l^{-1} (curve 1) and 0.15 mol l^{-1} (curve 2). Curve 3 is a blank voltamogram recorded with 0.15 mol l^{-1} chloride solution without the addition of Bi(III). Due to the complexation of Bi(III) with chloride, a shift of the peak potential towards negative values was observed. The change of the base current with the addition of chloride is the second, more important detail. This is caused by the oxidation of the mercury to calomel. The peak current determination of curve 1 is relatively simple, regardless of the method applied. However, the determination of the peak current from curve 2, is more difficult. The 'tangent fit' method is usually applied for the approximation of the linear base current (straight line T in curve 2), as well as the determination of the peak current from a straight line at the peak potential. In comparison to the peak current determined from the real base current, about a 20% smaller value is obtained.

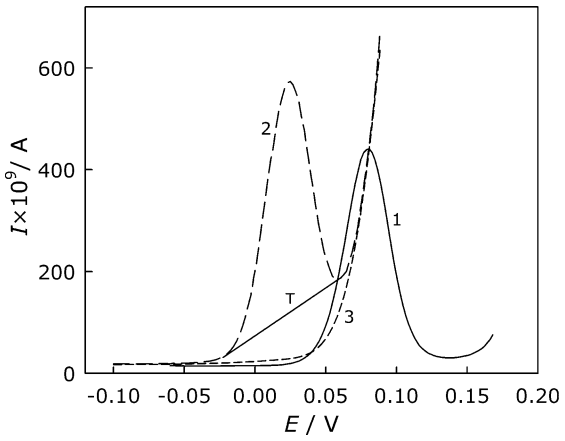

Fig. 9. The DPAS voltamograms of 2×10^{-7} mol l^{-1} Bi(III) in a $(1-x)$ mol l^{-1} $HClO_4 + x$ mol l^{-1} HCl. x: (1) 5×10^{-3} mol l^{-1} and (2) 0.15 mol l^{-1}. The curve 3 represents the base current of the blank electrolyte at a chloride concentration of 0.15 mol l^{-1} (without the addition of Bi(III)). (T) represents the baseline current used for the peak current determination by the 'tangent fit' method. The DPASV parameters: $E_{acc} = -0.15$ V, $E_i = -0.1$ V, $E_f = 0.18$ to 0.09 V, $E_{sc.inc} = -0.002$ V, $E_A = 0.025$ V, $t_{acc} = 120$ s, $t_{int} = 0.2$ s, $t_{mod} = 0.05$ s.

The effect of the peak current determination on the shape of the pseudopolarogram is illustrated in Fig. 10. Two pseudopolarograms of 2×10^{-7} mol l^{-1} Bi(III) (in supporting electrolyte of 0.85 mol l^{-1} $HClO_4 + 0.15$ mol l^{-1} HCl) are constructed using the 'tangent fit' method (curve 1) and the blank subtraction (curve 2). The pseudopolarograms are normalized for an easy comparison. The difference of the peak currents increases with the change of the accumulation potential towards positive values, i.e. with the diminishing of the absolute peak currents. The slope of the logarithmic line of curve 1 is steeper than expected for the three-electron charge transfer, while curve 2 is in agreement with the simulated

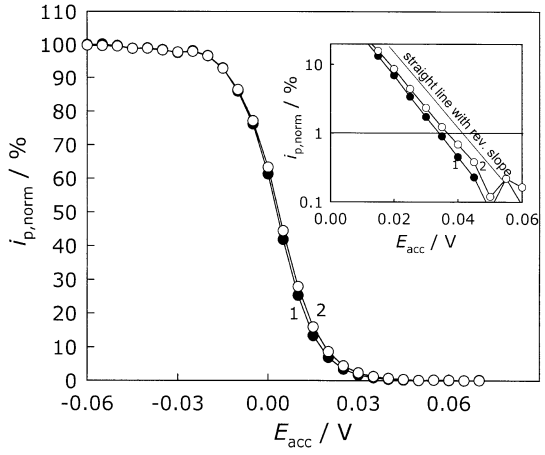

Fig. 10. The normalized pseudopolarograms of 2×10^{-7} mol l^{-1} Bi(III) at the constant ionic strength of 1 mol l^{-1} (0.85 mol l^{-1} $HClO_4 + 0.15$ mol l^{-1} HCl) constructed by the peak current determination using (1) a 'tangent fit' method and (2) a blank subtraction method. Inset: the fraction of the pseudopolarograms displayed on the logarithmic scale of the normalized peak currents.

pseudopolarogram. The inset of Fig. 10, which illustrates a part of the normalized currents of the pseudopolarograms on the logarithmic scale, shows that the potentials at 1% of the limiting current differ by about 3 mV. It is also evident that the peak currents of curve 2 follow the reversible slope below 1% of the limiting current, while the slope of curve 1 is steeper. This is very important because this range of the peak currents is used for the comparison of the experimental and the simulated pseudopolarograms, and the estimate of the formal potential of the quasireversible and irreversible redox reactions. Although the difference of the peak currents is about 20%, and the difference of the critical potentials 'only' 3 mV, such a systematic error will be incorporated in the final results of the evaluation of the trace metal speciation. The determination of the stability constants of the labile Bi(III) complexes with chloride using a classical DeFord–Hume approach [40], is an example of an appropriate determination of the peak currents which yields acceptable results.

The clarification of the experimental pseudopolarographic problems described is essential for further scientific research in the field of trace metal speciation. The pseudopolarography of the quasireversible and irreversible redox processes, and the speciation of the labile and inert metal complexes using a pseudopolarographic approach, will be elaborated.

4. Conclusions

Recently published papers show that pseudopolarography is a very useful method for the determination of the speciation of trace metals in model solutions and in natural waters at very low concentration levels. Since this method is very time-consuming, it is seldom used in electroanalytical research. The development of new software for the automated pseudopolarographic measurements (PSEUDOSOFT) using AUTOLAB instruments enabled autonomous pseudopolarographic measurements over several days. Using such an automated measurement system, an adequate number of data can be collected in a wide accumulation potential range, thus improving not only the statistical indicators but the accuracy of the final results, as well. The discrepancies between the experimental data as compared to those predicted theoretically, can be observed easily. This paper shows that proper data treatment provides good agreement between the polarographic and pseudopolarographic formal potentials. Using the proposed mathematical/graphical treatment of the pseudopolarographic data where the limiting current is not constant, reliable experimental and simulated data are obtained. The properly constructed pseudopolarograms are the basis for obtaining the accurate final results.

Acknowledgements

The authors wish to thank Milivoj Lovrić and Ivanka Pižeta for their helpful comments during the preparation of this manuscript. The financial support of the Ministry of Science and Technology of the Republic of Croatia, is gratefully acknowledged.

References

[1] S. Bubić, M. Branica, Thalassia Jugoslav. 9 (1973) 47.
[2] M. Branica, D.M. Novak, S. Bubić, Croat. Chem. Acta 49 (1977) 539.
[3] A. Zirino, S.P. Kounaves, Anal. Chem. 49 (1977) 56.
[4] M.S. Shuman, J.L. Cromer, Anal. Chem. 51 (1979) 1546.
[5] M. Lovrić, M. Branica, Croat. Chem. Acta 53 (1980) 485.
[6] S.P. Kounaves, Anal. Chem. 64 (1992) 2998.
[7] M. Lovrić, Electroanalysis 10 (1998) 1022.
[8] S.P. Kounaves, A. Zirino, Anal. Chim. Acta 109 (1979) 327.
[9] S.D. Brown, B.R. Kowalski, Anal. Chem. 51 (1979) 2133.
[10] A. Zirino, S.P. Kounaves, Anal. Chim. Acta 113 (1980) 79.
[11] L. Sipos, P. Valenta, H.W. Nürnberg, M. Branica, in: M. Branica, Z. Konrad (Eds.), Lead in the Marine Environment, Pergamon Press, Oxford, 1980.
[12] Š. Komorsky-Lovrić, M. Lovrić, M. Branica, J. Electroanal. Chem. 214 (1986) 37.
[13] Š. Komorsky-Lovrić, M. Branica, J. Electroanal. Chem. 226 (1987) 253.
[14] M. Vega, R. Pardo, M.M. Herguedas, E. Barrado, Y. Castrillejo, Anal. Chim. Acta 310 (1995) 131.
[15] M. Branica, I. Pižeta, I. Marić, J. Electroanal. Chem. 214 (1986) 95.
[16] D. Omanović, I. Pižeta, Ž. Peharec, M. Branica, Mar. Chem. 53 (1996) 121.
[17] R.M. Town, M. Fillela, J. Electroanal. Chem. 488 (2000) 1.
[18] G. Branica, M. Lovrić, Electrochim. Acta 42 (1996) 1247.
[19] B.L. Lewis, G.W. Luther, III, H. Lane, T.M. Church, Electroanalysis 7 (1995) 166.
[20] P. Croot, J.W. Moffet, G.W. Luther, III, Mar. Chem. 67 (1999) 219.
[21] D. Omanović, M. Branica, Croat. Chem. Acta 71 (1998) 421.
[22] D. Omanović, PhD thesis, University of Zagreb, Croatia, 2001.
[23] I. Pižeta, D. Omanović, M. Branica, Anal. Chim. Acta 331 (1996) 125.
[24] I. Ružić, J. Electroanal. Chem. 75 (1977) 25.
[25] A.J. Bard, L.R. Faulkner, Electrochemical Methods, Wiley, New York, 2001.
[26] A.M. Bond, R.D. Jones, Anal. Chim. Acta 121 (1980) 1.
[27] J.E. Anderson, A.M. Bond, R.D. Jones, J. Electroanal. Chem. 130 (1981) 113.
[28] D. Gonzalez-Arjona, G. Lopez-Perez, E. Roldan, J.D. Mozo, Electroanalysis 12 (2000) 1143.
[29] F. Vydra, K. Štulik, E. Julakova, Electrochemical Stripping Analysis, Ellis Horwood, Chichester, 1976.
[30] D.K. Roe, J.E.A. Toni, Anal. Chem. 37 (1965) 1503.
[31] M. Brand, I. Eshkenazi, E. Kirowa-Eisner, Anal. Chem. 69 (1997) 4660.
[32] W.R. Seitz, R. Jones, L.N. Klatt, W.D. Mason, Anal.Chem. 45 (1973) 840.
[33] D.L. Huizenga, D. Kester, J. Electroanal. Chem. 164 (1984) 229.
[34] J. Wang, J.M. Zadeii, J. Electroanal. Chem. 246 (1988) 297.
[35] A.M. Mota, M.M. Correia dos Santos, in: A. Tessier, D.R. Turner (Eds.), Metal Speciation and Bioavailability in Aquatic Systems, Wiley, New York, 1995.
[36] D. Krznarić, Mar. Chem. 15 (1984) 117.
[37] Š. Komorsky-Lovrić, M. Branica, Anal. Chim. Acta 276 (1993) 361.
[38] M. Lovrić, V. Svetlicić, V. Žutić, Electroanalysis 4 (1992) 963.
[39] I. Pižeta, D. Omanović, M. Branica, Anal. Chim. Acta 401 (1999) 163.
[40] D.D. DeFord, D.N. Hume, J. Am. Chem. Soc. 73 (1951) 5321.